



NUMERICAL MODELING OF EARTHQUAKE-INDUCED LIQUEFACTION EFFECTS ON SHALLOW FOUNDATIONS

K. Ziotopoulou⁽¹⁾, J. Montgomery⁽²⁾

⁽¹⁾ Assistant Professor, Department of Civil and Environmental Engineering, University of California, Davis, kziotopoulou@ucdavis.edu

⁽²⁾ Assistant Professor, Department of Civil Engineering, Auburn University, jmontgomery@auburn.edu

Abstract

Liquefaction continues to be a major source of damage to structures during earthquakes (e.g., Canterbury earthquake sequence, New Zealand [1]). Liquefaction and subsequent reconsolidation can lead to settlement, ground cracking and loss of bearing capacity all of which can cause damage to structures. The ability of engineers to design against this type of damage requires methods which can evaluate the potential for liquefaction-induced damages and how these will be affected by varying field conditions (e.g., seismic motion, soil profile and building properties). Current practice primarily relies on empirically developed charts which correlate post-liquefaction settlement to the relative density of sand or the surface manifestation of liquefaction to the relative thickness of non-liquefiable crust layer to the liquefiable one. Despite their widespread use, these charts are based on a small number of case histories and do not directly account for other factors such as the thickness of the liquefiable layer, properties of the non-liquefiable crust and effects of a building. The limited ability of current design procedures to predict and account for such effects emphasizes the need to develop a more rational approach towards accounting for these phenomena and incorporating them into the design of shallow foundations.

This paper evaluates the effects of post-liquefaction reconsolidation settlements on shallow foundations using numerical simulations. Two-dimensional, fully coupled dynamic analyses are used to simulate the response of shallow foundations on liquefiable soil deposits. The baseline analysis is first validated against two selected cases of a centrifuge test and the efficacy of our current tools (numerical platform and constitutive model for liquefiable soil) in capturing the trends observed in the centrifuge tests is investigated. The validated analysis is then used to investigate more factors which may have an effect on the settlement patterns such as the crust layer thickness, soil properties, and bearing pressure. Implications for practice are discussed.

Keywords: liquefaction; numerical modeling; post-liquefaction reconsolidation; settlements; shallow foundations



1. Introduction

Observations in recent earthquakes have emphasized the major role liquefaction of sandy soils plays in damage to structures (e.g., [2]). Liquefaction and subsequent reconsolidation can lead to settlement, ground cracking and loss of bearing capacity all of which can cause damage to structures. Numerous researchers (e.g., [3 – 9]) have worked on the experimental and numerical evaluation of such effects on structures and have provided valuable insights to the aforementioned mechanisms. The potential for damage due to liquefaction is also often evaluated using empirically developed charts which correlate the magnitude of potential post-liquefaction settlement to the relative density of the deposit (e.g., [10]) or the surface manifestation of liquefaction to the relative thicknesses of the non-liquefiable crust and the liquefiable layer (e.g., [11]). Subsequent authors have combined these methods into liquefaction severity indices (e.g., LPI [12], LPI_{ish} [13], LSN [14]) which can be correlated to the potential for liquefaction-induced damage at a given site. Despite their widespread use, these charts are based on a small number of case histories and do not directly account for other factors such as the properties of the non-liquefiable crust or the effects of a structure.

Centrifuge modeling has been used to investigate some of the other factors which affect the potential for liquefaction-induced settlement of structures with shallow foundations. Dashti et al. ([6]) performed a suite of centrifuge tests to gain insight into the seismic performance of buildings with rigid mat foundations on a relatively thin deposit of liquefiable, clean sand. The relative density and thickness of the liquefiable layer as well as the structural properties were varied to identify the key parameters affecting soil and structural response and the primary mechanisms involved in liquefaction-induced building settlement. Their primary conclusion was that settlement of structures with shallow foundations was due primarily to deviatoric strains induced during shaking, with volumetric strains due to reconsolidation of the liquefied layer being relatively less important. This trend was reversed for free-field conditions illustrating the important role the weight of the structure plays in the response. The authors indicated that the relative importance of these settlement mechanisms is likely to strongly depend on the properties of the ground motion, soil and structure.

This paper seeks to evaluate the relative importance of post-liquefaction reconsolidation settlements on shallow foundations using numerical simulations. The results of a validation study of numerical simulations against selected centrifuge tests are presented first. The setup of the numerical simulation along with the calibration of the constitutive model are described, followed by the results of the validation exercise. The validated analysis provides the basis for a parametric investigation of selected parameters. The paper concludes with a summary of observations and insights gained.

2. Description of Centrifuge Tests

Two tests (SDH01 and SDH02) by Dashti et al. ([6]) were selected as the basis of comparisons between numerical simulations and centrifuge tests. Curated data were obtained from the FLIQ: Foundation and Ground Performance in Liquefaction Experiments ([15], Events 5, 9, 13 and 21, 25, 29) database. Fig. 1 and Table 1 summarize the configuration and properties of the tests that are of interest for this paper. The models were spun at a nominal centrifuge acceleration of 55g, and unless indicated otherwise, all units used in this paper are in prototype scale. The two tests referred to (herein and in [6]) as T3-30 and T6-30 included a liquefiable soil layer of Nevada Sand with a prototype thickness H_L of 3 m and 6m respectively and a nominal relative density D_R of 30% or 40%. The liquefiable layer of loose Nevada sand is underlain by a thick layer of dense Nevada sand with a nominal relative density D_R of 90% and 86% respectively and a thickness of 21m and 18 m respectively. The loose Nevada sand is also overlain by a 2 m thick layer of dense Monterey sand, while the water table is located at 1.1 m deep. The same series of realistic earthquake motions were applied to the base of the model consecutively in both experiments of interest. Sufficient time between shakes was allowed to ensure full dissipation of excess pore pressures. The input motions included a sequence of scaled versions (small, moderate, and large) of the north-south, fault-normal component of the 1995 Kobe Port Island motion.

3. Validation of Numerical Simulations

The numerical simulation of the response of one of the structures of SDH01 was performed using the commercial, finite difference software FLAC 7 ([16]). The information provided in this section, combined with the FLAC 7 manual ([16]) and the PM4Sand Version 3 manual ([14]) are sufficient for recreating the analyses presented herein. The goal of the analysis was to validate the numerical simulation against the recorded experimental results and obtain a satisfactory agreement between the two. The validated numerical simulation was utilized to perform a parametric investigation on selected properties of the model, and investigate their effect on the obtained response.

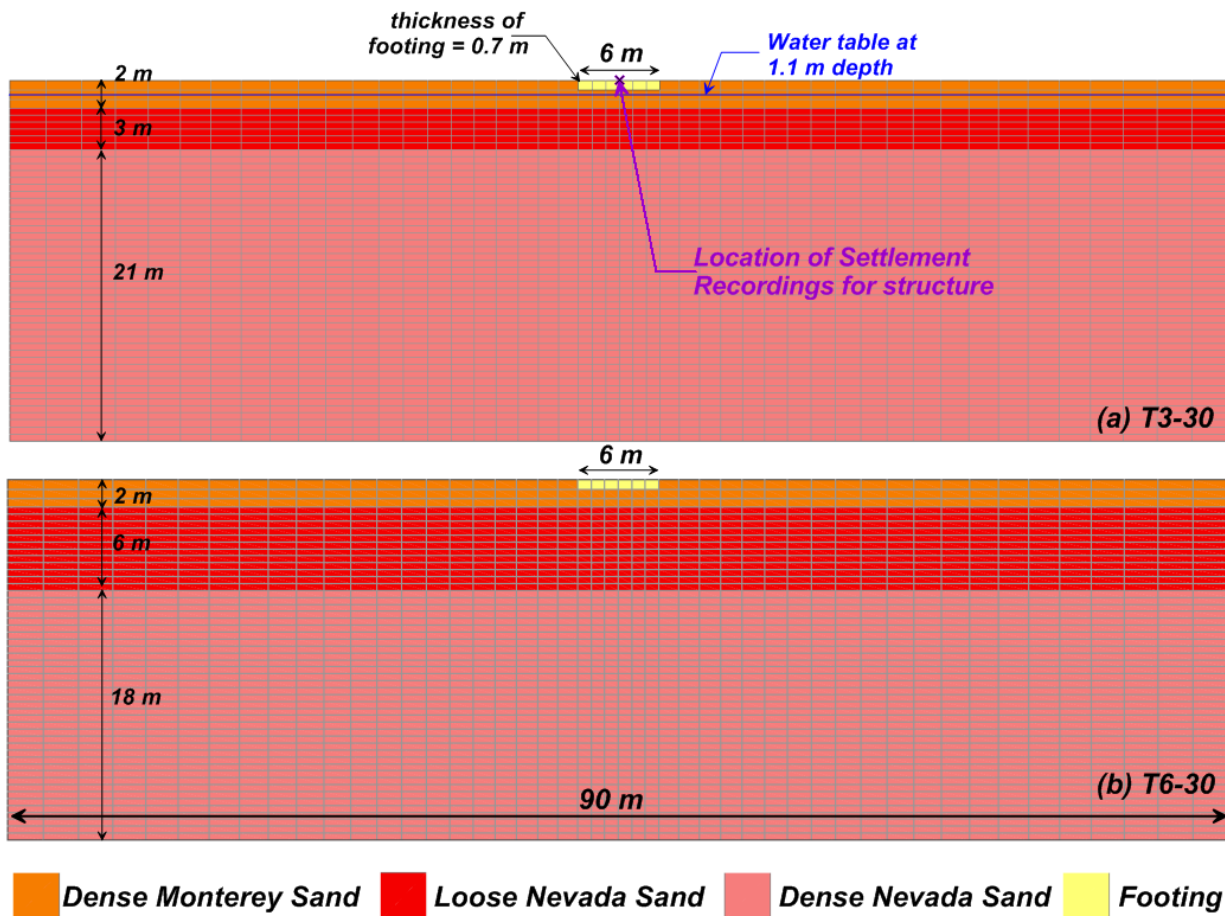


Fig. 1 – Numerical grid and components of the T3-30 and T6-30 experiment simulations.

3.1 Numerical model

The numerical simulations are performed for the prototype problem (Fig. 1). The numerical grid (Fig. 1) consists of the three uniform layers of sand with a total model thickness of 26m and width of 90m to reduce the influence of the boundaries on the response of the footing. FLAC uses four-node quadrilateral elements or zones with a mixed discretization scheme as described in detail in the manual ([16]). The numerical model for these tests contained 48 zones in the horizontal direction and 51 zones in the vertical leading to a total of 2448 zones. The grid was refined in the region closer to the embedded footing and gradually coarsened towards the left and right boundaries to provide a better discretization in the area of interest. All soil layers were modeled with the PM4Sand Version 3 constitutive model ([17]) as described in the next section. The rigid footing was modeled as six elastic zones (6 m wide in total) with properties corresponding to the reported geometry, mass, and stiffness properties reported in the FLIQ database ([15]). The dynamic properties of the superstructure were not considered under the assumption that for the selected relatively short-period structures (type A and B per the FLIQ database), these



effects will be negligible. Unglued interface elements were applied between the footing and the surrounding soil to account for the frictional interaction between the two. A friction and dilation angle of 33 degrees and 0 degrees respectively were assigned and slip was allowed. Within the code, the interface is represented as a series of normal and shear springs that connect the opposing surfaces at interacting nodes. The corresponding normal and shear stiffnesses of the springs were both set to $2e7 \text{ Pa/m}$. The footing bearing pressure was applied as a distributed force to the nodes along the top of the footing zones.

There are two possible approaches for running simulations of consecutive shaking events: (1) simulate all shakes in sequence with sufficient time for dissipation between them (as occurred in the centrifuge test itself) or (2) simulate each shake individually using a newly generated mesh with a best estimate on the geometry and other properties at the beginning of that shaking event in the test. Kamai and Boulanger ([18]) explored both options and concluded that although both approaches can yield comparable results in terms of the dynamic response and the final deformations, the former one is more accurate in tracking the progressive and cumulative effects of shaking. This approach was employed herein and the three shaking events recorded in the North-South direction and reported in the FLIQ database were consecutively applied as acceleration time histories.

The boundary conditions for the model consisted of fixing the nodes along the base of the model in both the horizontal and vertical directions. During shaking simulations, the desired ground motion was applied as a horizontal acceleration to the bottom nodes. Displacements of nodes along the sides of the model were tied together with the corresponding node along the opposite side to reflect the constraints imposed by the model container. All simulations included coupled fluid and mechanical calculations. The sides and bottom of the model were considered no flow boundaries to simulate the effects of the container while drainage was allowed through the surface of the model.

3.2 Calibration of constitutive model

The PM4Sand model (Version 3) has 22 input parameters, from which only three are considered primary and are required as model input. These are the initial relative density (D_R), the shear modulus coefficient (G_o) used to define the elastic shear modulus, and the contraction rate parameter (h_{po}) used for calibration of the undrained shear strength. The other 19 (2 flags and 17 secondary parameters) can be either left with their preset default values, that are generally functions of an index property, if no other information is available, or calibrated to the desired response based on the available lab data. For this study, the two primary parameters D_R and h_{po} were set and calibrated respectively using the experimental data for Nevada and Monterey Sand ([16]). The shear modulus coefficient (G_o) was calculated as a function of relative density according to the following relationship as suggested by Boulanger and Ziotopoulou ([17]):

$$G_o = 167\sqrt{(N_1)_{60} + 2.5} \quad (1)$$

where:

$$(N_1)_{60} = \sqrt{\frac{D_R}{46}} \quad (2)$$

Table 1 lists the final calibration parameters used for the sand material (other parameters and their default values, listed in [17], are omitted for brevity).

Two model properties were adjusted to provide a better match to the centrifuge tests (Class C prediction, [19]). Preliminary simulations for this paper showed that the simulated strengths for the soils appeared to be lower, and the rate of reconsolidation appeared to be slower than was observed in the experiments. As a result, the cyclic resistance ratios (CRRs) used in these simulations for the loose Nevada sand layers (Table 1) are approximately 25% larger than those reported by Karimi and Dashti ([20]). The permeability is also approximately twice as large



as the target value for these tests ([21]). These adjustments are considered to be relatively minor considering the potential uncertainties between the results from laboratory tests and the as-placed soil properties in the centrifuge.

PM4Sand incorporates a phenomenological formulation to provide more realistic estimates of the reconsolidation volumetric strains that develop during the post-shaking portion of a numerical simulation. This involves the reduction of the post-shaking elastic shear modulus G (and hence the elastic bulk modulus K) which increases reconsolidation strains, thereby compensating for the sedimentation strains which are not explicitly modeled in the elastic or plastic components of the constitutive model. This feature can be activated after the end of strong shaking, such that post-liquefaction reconsolidation strains are better approximated in the remainder of the simulation. After each shaking event, the PostShake flag of PM4Sand was turned on and the model was allowed to reconsolidate for approximately 6 hours of flow time to allow excess pore pressures to dissipate.

Table 1 – Soil properties utilized in the numerical simulations

Property	Nevada Sand		Dense Monterey Sand
	Loose	Dense	
D_R	30 % (T3-30) 40 % (T6-30)	90 %	86 %
Cyclic Resistance Ratio CRR	0.04 (reported by Karimi and Dashti 2016) 0.05 (implemented herein) 0.08 (reported by Karimi and Dashti 2016) 0.1 (implemented herein)	0.36	0.44
G_S	2.67		2.64
$\gamma_{d,max}$	17.02 kN/m^3		16.81 kN/m^3
$\gamma_{d,min}$	13.98 kN/m^3		13.96 kN/m^3
γ_{sat}	19.2 kN/m^3	20.2 kN/m^3	19.9 kN/m^3
Permeability	0.0035 cm/sec		–
Contraction Rate Parameter h_{po}	0.055 0.48	0.06	0.56
Shear Modulus Coefficient G_o	427 528.5	1162	1092

4. Results

Results between the numerical simulations and centrifuge tests were compared primarily in terms of settlement of the footing. As previously discussed, the three shaking events were run in succession with time in between each event for reconsolidation to occur. The centrifuge tests included a small step wave prior to the suite of Port Island motions which was not included in the numerical simulations. Incremental (per event) and cumulative settlement results are reported in Table 2 for the center of the footing (Fig. 1) along with the observed settlements from the

centrifuge models as reported in the FLIQ database. The time history of incremental footing displacement from the numerical simulation is compared with the centrifuge data for the Large Port Island motion in Figure 2.

Table 2 – Comparison between experimental and numerical values of vertical settlements of the footing for the two simulated centrifuge tests.

Test	Motion (PI stands for Port Island)	CENTRIFUGE		NUMERICAL SIMULATION	
		Incremental Settlement of the Structure (mm)	Cumulative settlement of the structure up to & including the event (mm)	Incremental Settlement of the Structure (mm) recorded at the center of the footing	Cumulative settlement of the structure up to & including the event (mm)
T6-30 (Fig. 1a)	Small PI	2.3	4.8*	4.0	4.0
	Moderate PI	80	84.8	249.2	253.2
	Large PI	592.9	677.7	626.0	879.2
T3-30 (Fig. 1b)	Small PI	2.1	3.5*	30.6	30.6
	Moderate PI	283.7	287.2	288.3	318.9
	Large PI	500	787.2	556.9	875.8

*includes settlements experienced during a small Step motion applied before the Small PI one.

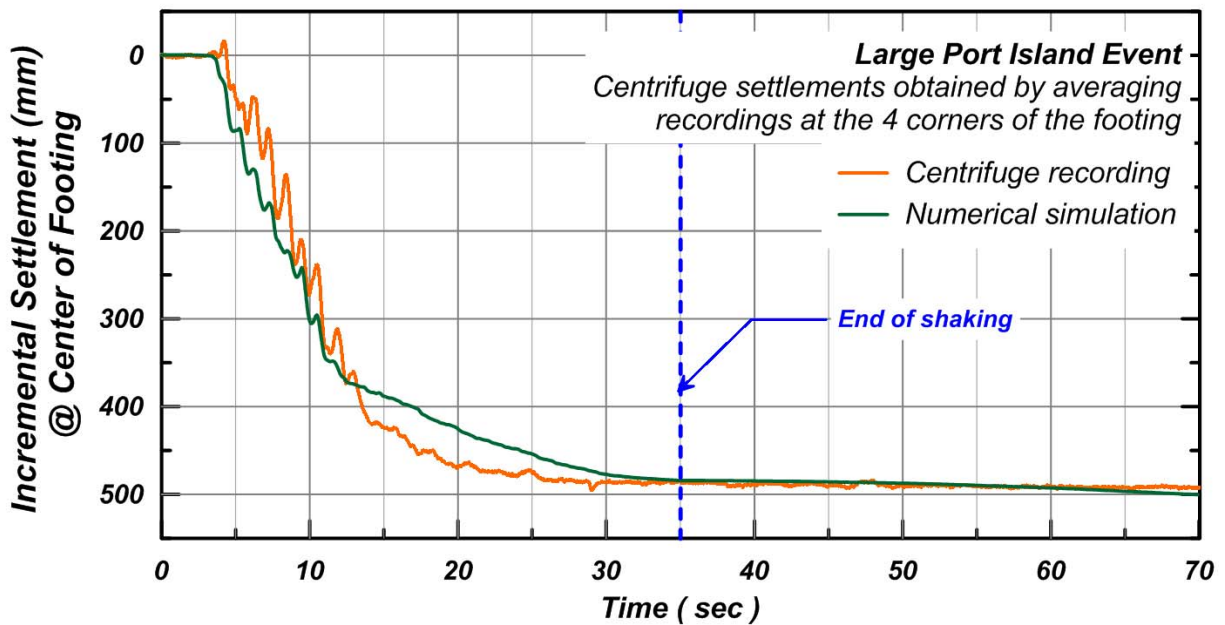


Fig. 2 – Numerical and experimental settlement time histories of the footing in T3-30 during the Large Port Island Shaking event.

Incremental settlement results (Table 2) for the T6-30 simulation are in relatively close agreement with the centrifuge test for the small and large Port Island motions, but are significantly higher for the moderate event. This leads to a corresponding overprediction in final cumulative settlements. Incremental settlement results for the T3-



30 are in relatively close agreement with the centrifuge test results for the moderate and large Port Island motions, but significantly larger for the small motion. This again leads to a corresponding overprediction in the cumulative settlements.

The rate of settlement can also be compared for the numerical simulation and the centrifuge tests (Fig. 2). The footing in the numerical simulation shows less dynamic response than was observed in the centrifuge test which may be due in part to the lack of a structure in the numerical simulations. The numerical simulations also show a smaller settlement rate than was observed in the centrifuge test which may be improved with further refinement of the permeability values or consideration of potential changes in permeability during shaking. The numerical simulation continues to settle after the end of shaking as the soil continues to reconsolidate while the centrifuge simulation shows less settlement after the end of shaking. This difference may be due in part to differences in permeability and the limitations of the current simulation which consider the dynamic shaking and reconsolidation sequentially.

The validation results show that at lower shaking levels the numerical model is overpredicting the extent of liquefaction in the loose sand layers relative to the observations in the centrifuge test. For the large event, the majority of the layer is generating excess pore pressures and the centrifuge and numerical simulations are in relatively close agreement. The agreement at lower shaking levels could likely be improved through a more detailed calibration, but as the focus of this paper is on the response once liquefaction has been triggered, this refinement did not seem warranted. Given the overall uncertainty of geotechnical experiments as well as the limitations of the numerical simulations performed (e.g. two-dimensional plane strain), these validation results were considered satisfactory for the scope of the herein presented work.

4.1 Parametric Investigation

Based on the validated simulations presented in the previous section, a parametric investigation was performed to explore parameters that are rationally expected to be guiding the behavior of the system. The parameters explored herein were: thickness of the non-liquefiable layer of dense Monterey Sand (2 m, 4 m, and 6 m), thickness of the loose liquefiable Nevada sand (3 m, 6 m and 9 m), footing width (6m and 12m), bearing pressure (60 kPa, 80 kPa, and 120 kPa), and relative density of the liquefiable loose Nevada Sand (30% and 40%). All other parameters and properties of the numerical simulation were preserved identical to those of the validated baseline case. Each of the parametric runs was performed using the large Port Island motion.

4.2 Results and Observations

Two response measures were examined in this parametric study. The first is the total settlement of the footing normalized by the thickness of the liquefiable layer (Fig. 3 and 4). The second response measure was the contribution of reconsolidation settlement (settlement occurring after shaking) expressed as a percentage of the total settlement (Fig. 4 and 5).

Fig. 3 and Fig. 4 illustrate the amount of total settlement normalized by the thickness of the liquefiable layer versus the three magnitudes of bearing pressure. Different symbols are used to indicate the three different crust layer thicknesses. Fig. 3 shows the results using a footing width of 6 m while Fig. 4 shows the results for a footing width of 12 m. For all cases, the normalized total settlement generally increases with increasing bearing pressure. This effect is more pronounced for the narrower footing (Fig. 3) and for the lower relative density (Fig. 3b and Fig. 4b). The results also show that the lower relative density layer lead to larger normalized settlements. These observations are consistent with the trends noted by Dashti et al. ([6]). The role of the thickness of the non-liquefiable crust was not explored by Dashti et al. ([6]), but can be observed in Fig. 3 and Fig. 4. The normalized settlement generally increased as the crust layer thickness decreased which is consistent with the general trend noted by Ishihara ([11]). This effect was more pronounced for the lower relative density and heavily loaded footings as also observed by Karamitros et al. ([7]). The crust layer thickness has the largest effect on the normalized settlement of the parameters examined.

Fig. 5 and Fig. 6 illustrate the amount of settlement due to post-liquefaction reconsolidation versus the three magnitudes of bearing pressure and versus the non-liquefiable layer thickness respectively, for all cases examined. For each case, three points are shown for the three liquefiable layer thicknesses. Fig. 5 shows the results for footing width of 6 m while Fig. 6 shows the results for a footing width of 12 m. For both cases, the contribution of reconsolidation to total settlement decreases with increasing bearing pressure and decreasing crust layer thickness. The contribution is lowest for thin crusts and heavily loaded footings which is consistent with the observations of Dashti et al. ([6]) and Karamitros et al. ([7]). The contribution of reconsolidation settlements also generally increased with decreasing relative density and footing width, but these effects were less significant than the bearing pressure or crust layer thickness.

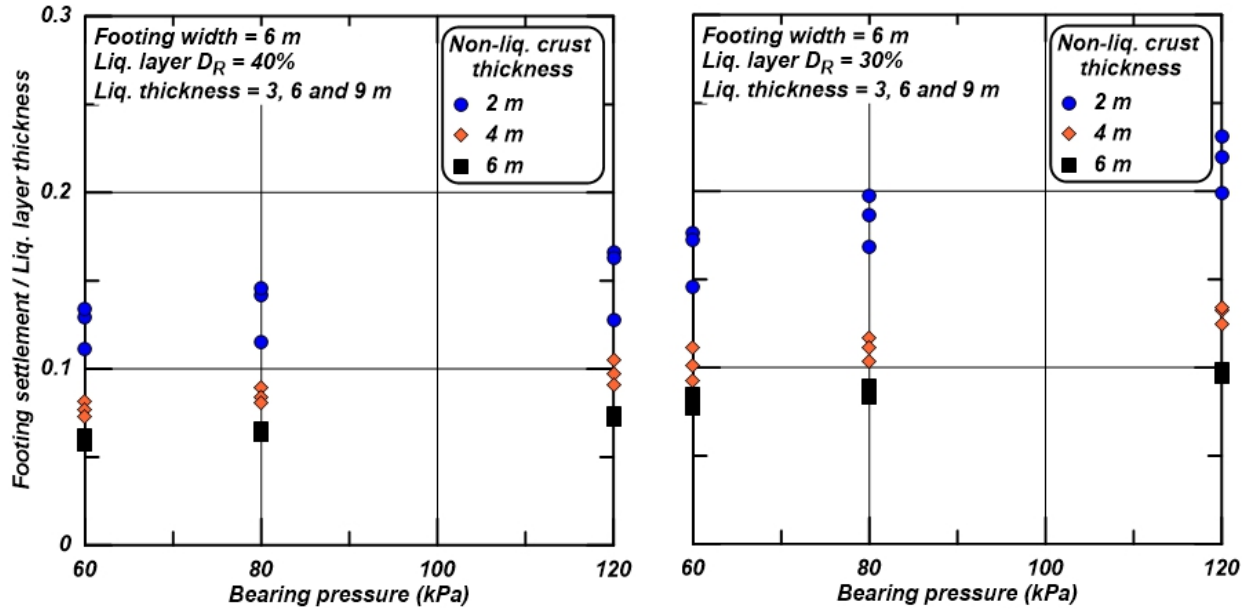


Fig. 3 – Total footing settlement normalized by the thickness of the liquefiable (liq.) layer for a 6 m wide footing shown versus bearing pressure for three crust thickness and three liquefiable layer thicknesses. Each set of identical data points per x-intercept (bearing pressure) corresponds to the three shaking events.

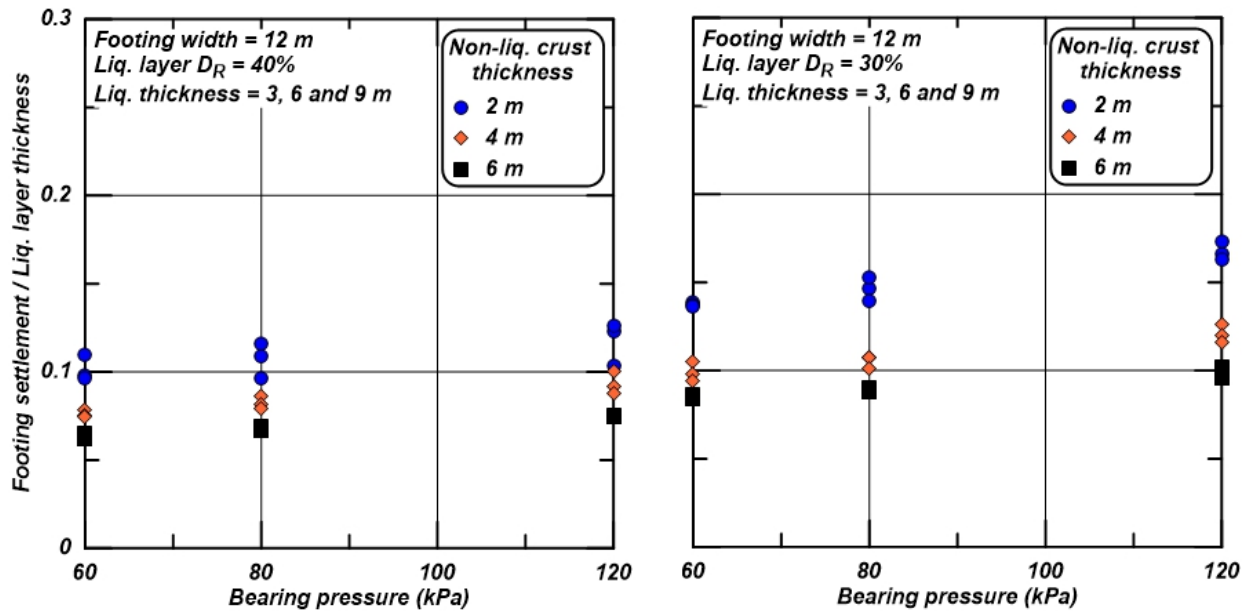


Fig. 4 – Total footing settlement normalized by the thickness of the liquefiable (liq.) layer for a 12 m wide footing shown versus bearing pressure for three crust thickness and three liquefiable layer thicknesses.

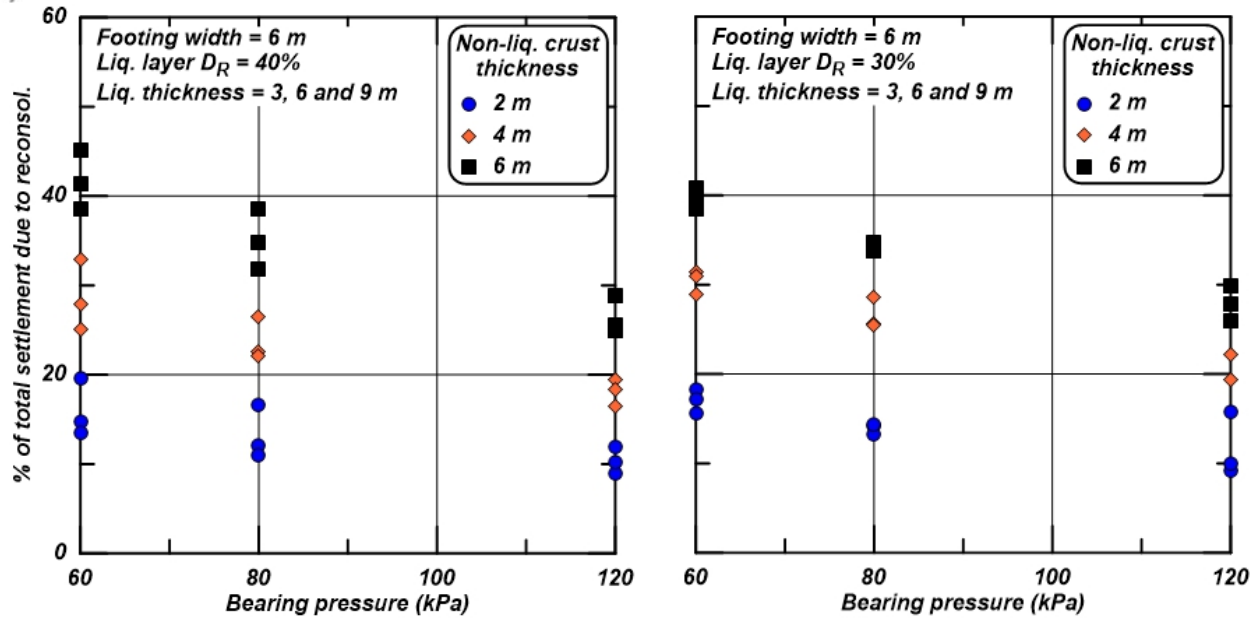


Fig. 5 – Percentage of total settlement due to post-shaking reconsolidation for a 6 m wide footing shown versus bearing pressure for three crust thickness and three liquefiable layer thicknesses.

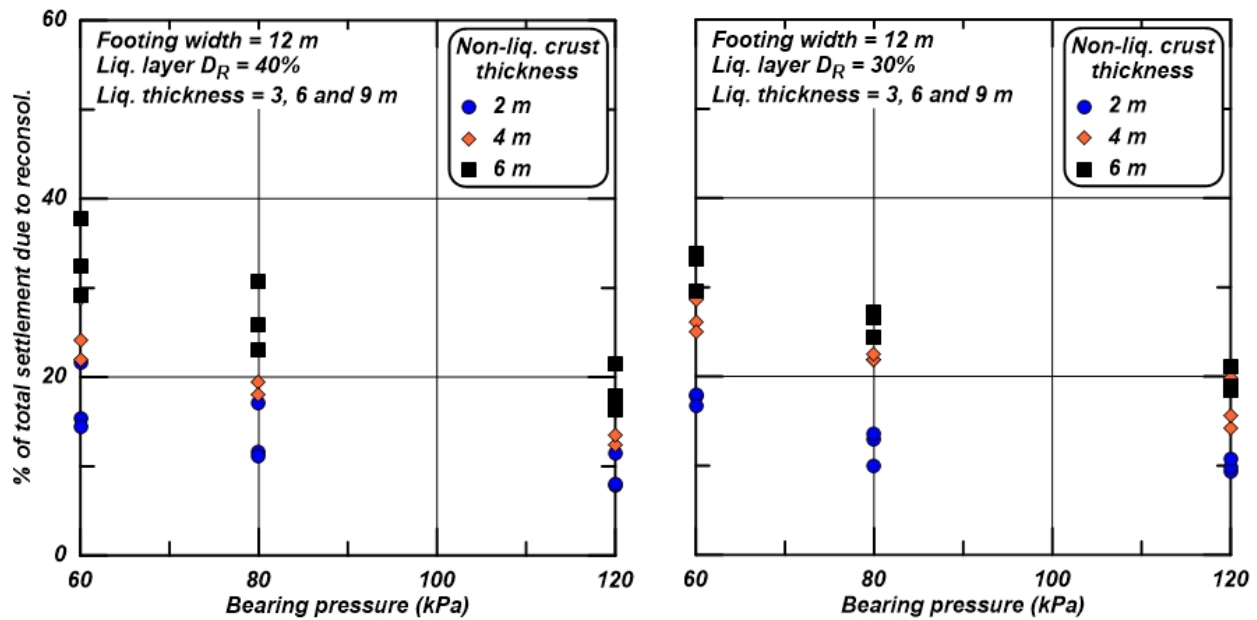


Fig. 6 – Percentage of total settlement due to post-shaking reconsolidation for a 12 m wide footing shown versus bearing pressure for three crust thickness and three liquefiable layer thicknesses.

5. Conclusions and Future work

The goal of this paper was to evaluate the relative importance of post-liquefaction reconsolidation settlements on shallow foundations using numerical simulations. Two selected centrifuge tests investigating the response of shallow foundations on liquefiable soil were numerically simulated and the results were validated against the experimental observations. The validated analyses provided the basis for the parametric investigation of the effects of selected parameters (bearing pressure, footing width, thickness of non-liquefiable crust) on the obtained settlements.



The findings of the parametric investigation were in general agreement with those by other researchers ([6] and [7]). Settlements primarily accumulated for as long as the shaking continued while a relatively smaller portion of settlements developed during the post-liquefaction phase when excess pore pressures dissipated. Thus, most of the total footing settlements were generated during strong motion shaking due to deviatoric settlement with a comparatively smaller portion of the settlement due to post-liquefaction reconsolidation volumetric strains. The deviatoric strains are likely due to both loss of strength due to partial bearing failure and accumulation of settlements due to soil-structure-interaction (ratcheting), as discussed by Dashti et al. ([6]). Increasing the footing width reduced the overall magnitude of settlement for the thinner crust, but had a smaller effect for other crust thicknesses. Reconsolidation strains tended to make up a larger percentage of the overall settlement for lightly loaded footings and thicker crusts.

Further investigation is needed in order to elucidate more aspects of the response (accelerations, lateral displacements, and pore pressures) towards advancing the performance-based evaluation of liquefaction effects on shallow footings. Thus, a refined Class C prediction targeting at all the aforementioned response metrics will provide further insights. The constitutive model utilized herein, phenomenologically accounts for the combined effects of reconsolidation strains and as such does not explicitly account for the separate mechanisms of sedimentation and self-weight reconsolidation. As such, the separate effects of these two mechanisms on the structures cannot be accounted for without a different constitutive formulation and this could also be a topic of future studies. In addition, the two-dimensional simulation of a three-dimensional problem has introduced some simplifications. Three-dimensional simulations would be capable of capturing several effects better (e.g. dissipation of pore pressures, shape of footing, and the dynamic characteristics of the structures) which could not be incorporated in the analyses presented herein. Future work could also include more refined laboratory investigation of soil properties which will facilitate better calibration of the advanced constitutive models for liquefiable soils.

6. Acknowledgements

The authors would like to thank Dr. Zana Karimi and Professor Shideh Dashti (CU Boulder) who provided valuable assistance with the centrifuge test data of the Dashti et al. (2010) tests.

7. References

- [1] Tonkin & Taylor. (2012): Canterbury earthquakes 2010 and 2011-Land report as of 29 February 2012. New Zealand Earthquake Commission.
- [2] Bray J, Cubrinovski M, Zupan J, Taylor M (2014): Liquefaction Effects on Buildings in the Central Business District of Christchurch. *Earthquake Spectra*, **30**(1), 85-109.
- [3] Liu L, Dobry R (1997): Seismic response of shallow foundation on liquefiable sand. *Journal of Geotechnical and Geoenvironmental Engineering*, **123**(6), 557-567.
- [4] Naesgaard E, Byrne PM, Ven Huizen G (1998): Behaviour of light structures founded on soil crust over liquefied ground. *Geotechnical Earthquake Engineering and Soil Dynamics III- Geotechnical Special Publication*, **75**, 42-433.
- [5] Shahir H, Pak A (2010): Estimating liquefaction-induced settlement of shallow foundations by numerical approach. *Computers and Geotechnics*, 267-279. doi:10.1016/j.compgeo.2009.10.001
- [6] Dashti S, Bray JD, Pestana JM, Riemer MR, Wilson D. (2010): Mechanisms of Seismically-Induced Settlement of Buildings with Shallow Foundations on Liquefiable Soil. *Journal of Geotechnical and Geoenvironmental Engineering*, ASCE, **136** (1), 151-164.
- [7] Karamitros D, Bouckovalas G, Chaloulos Y (2013) Insight into the Seismic Liquefaction Performance of Shallow Foundations. *Journal of Geotechnical and Geoenvironmental Engineering*, **139**(4), 599-607
- [8] Asgari A, Golshani A, Bagheri M (2014): Numerical evaluation of seismic response of shallow foundation on loose silt and silty sand. *Journal of Earth System Science*, **123**(2), 365-379.
- [9] Qin J, Zeng X, Ming H (2015): Centrifuge modeling and the influence of fabric anisotropy on seismic response of foundations. *Journal of Geotechnical and Geoenvironmental Engineering*. doi:10.1061/(ASCE)GT.1943-5606



- [10] Ishihara K, Yoshimine M (1992): Evaluation of settlements in sand deposits following liquefaction during earthquakes. *Soils and Foundations*, 32(1), 173-188.
- [11] Ishihara K (1985): Stability of natural deposits during earthquakes. 11th International Conference on Soil Mechanics and Foundation Engineering, 321-376, San Fransisco, August 12-16.
- [12] Iwasaki T, Tokida K, Tatsuko F, Yasuda S (1978): A Practical Method for Assessing Soil Liquefaction Potential Based on Case Studies at Various Sites in Japan. *Proceedings of 2nd International Conference on Microzonation*, San Francisco, 85–896, 1978.
- [13] Maurer BW, Green RA, Taylor O-D (2015): Moving towards an improved index for assessing liquefaction hazard: lessons from historical data. *Soils and Foundations*, **55**(4): 778–787
- [14] van Ballegooy S, Malan P, Lacrosse V, Jacka M, Cubrinovski M, Bray JD, O'Rourke TD, Crawford SA, Cowan H (2014): Assessment of Liquefaction induced Land Damage for Residential Christchurch, *Earthquake Spectra*, February 2014, **30**(1), 31–55.
- [15] Allmond JD, Kutter BL, Bray J, Hayden C. (2014): New Database for Foundation and Ground Performance in Liquefaction Experiments. *Data Paper. Earthquake Spectra*, 31(4), 2485–2509.
- [16] Itasca (2011): *FLAC – Fast Lagrangian Analysis of Continua*, Version 7.0, Itasca Consulting Group, Inc., Minneapolis, Minnesota.
- [17] Boulanger RW, Ziotopoulou K. (2015): *PM4Sand (Version 3): A sand plasticity model for earthquake engineering applications*. Report No. UCD/CGM-15/01, Center for Geotechnical Modeling, University of California, Davis, CA, 2015, 112 pp.
- [18] Kamai R, Boulanger RW (2013): Simulations of a Centrifuge Test with Lateral Spreading and Void Redistribution Effects. *Journal of Geotechnical and Geoenvironmental Engineering*, ASCE, 139(8), 1250-1261.
- [19] Lambe TW (1973): Predictions in Soil Engineering. *Géotechnique*, 23(2), 149–202.
- [20] Karimi Z, Dashti S (2016): Seismic Performance of Shallow Founded Structures on Liquefiable Ground: Validation of Numerical Simulations Using Centrifuge Experiments. *Journal of Geotechnical and Geoenvironmental Engineering*, ASCE, ASCE, DOI: 10.1061/(ASCE)GT.1943-5606.0001479.
- [21] Dashti S, Bray JD, Riemer MR, Wilson D. (2009): *Centrifuge Data Report for Test Series SHD01*. Report No. UCB/CGMDR-08/06, Dept. of Civil and Environmental Engineering, University of California, Berkeley, CA, 46 pp.